# ChemComm

Accepted Manuscript


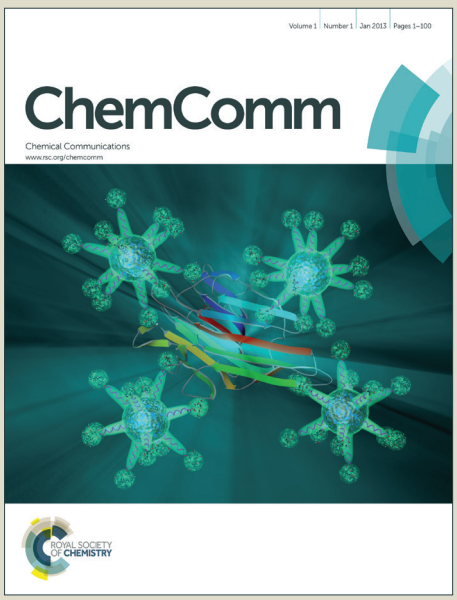





ROYAL SOCIETY OF CHEMISTRY

www.rsc.org/chemcomm

Journal Name

RSCPublishing

COMMUNICATION

# Transparent conducting p-type thin films of c-axis self-oriented $Bi_2Sr_2Co_2O_y$ with high figure of merit

Cite this: DOI: 10.1039/x0xx00000x

Renhuai Wei,[a] Xianwu Tang,[a] Ling Hu,[a] Zhenzhen Hui,[a] Jie Yang,[a] Hongmei Luo,[b] Xuan Luo,[a] Jianming Dai,[a] Wenhai Song,[a] Zhaorong Yang,[a] Xuebin Zhu*[a] and Yuping Sun*[ac]

Received 00th xxxxxxx 201x,
Accepted 00th xxxxxxx 201x

DOI: 10.1039/x0xx00000x

www.rsc.org/

**Transparent conducting p-type $Bi_2Sr_2Co_2O_y$ thin films have been first grown on $SrTiO_3$ substrates by a chemical solution deposition, showing c-axis self-orientation. The figure of merit can reach as high as 800 $M\Omega^{-1}$, which is the highest value for p-type transparent conducting thin films by solution methods.**

Nowadays transparent conducting oxides (TCOs) are widely used in many applications such as electrodes and coatings. However, most of the TCOs are n-type semiconductors such as ZnO: Al and indium tin oxide (ITO).[1–3] To date the reports on p-type TCOs are relatively rare. The figure of merit $FOM = -1/(R_{sh} \times \ln T)$,[4] where $R_{sh}$ and $T$ are the sheet resistance and average transmittance respectively, is very small as compared with that of the n-type TCOs.[5–8] To develop a type of p-type TCO with high *FOM* is very critical to explore the potential applications of TCOs. Layered cobaltates, consisting of blocking layers and $CdI_2$-type $CoO_2$ layers, have been progressing largely in recent years due to their p-type thermoelectric properties.[9] As similar to the $SrTiO_3$-based TCOs such as $SrTi_{1-x}Sb_xO_3$,[10] the layered cobaltates also show strong electrical correlation properties,[11,12] and the carrier mobility for these two materials is about 1 $cm^2/V$ s. [10,13] The similar properties between $SrTiO_3$-based TCOs and the layered cobaltates suggest that the layered cobaltates may be suitable to be used as p-type TCOs and have been reported recently.[14]

In order to optimize the properties in layered cobaltates, it is necessary to fabricate c-axis oriented thin films due to the anisotropy in these materials.[15,16] Fortunately, in our previous reports we first reported the interesting characteristics of self-assembled c-axis orientation in layered cobaltates thin films including $Ca_3Co_4O_9$, $Bi_2Sr_2Co_2O_y$ (BSC222) as well as $Bi_2Sr_3Co_2O_y$ derived by chemical solution deposition methods.[17,18] In this communication, BSC222 thin films are first reported as a novel p-type TCO by a chemical solution deposition, which is scalable for preparation. The *FOM* can reach as high as 800 $M\Omega^{-1}$, which is the highest value for p-type transparent conducting thin films by solution methods.

Figure 1 shows the high-resolution X-ray diffraction (HR-XRD) patterns for all derived BSC222 thin films on different $SrTiO_3$ (STO) substrates using a monochromatic Cu-$K_\alpha$ radiation. It is worth noting here that all BSC222 thin films are purely c-axis oriented regardless of the substrate orientation, suggesting the self-orientation of the derived BSC222 thin films. The calculated c-axis lattice constant is about 14.9 Å for all BSC222 thin films, which is same as our previous reports indicating the stoichiometry for all derived thin films.[17,19] Moreover, rocking curve measurements are carried out to determine the quality of out-of-plane orientation, and the results are shown in the insets of Fig. 1. It can be seen that the full width at half maximum (FWHM) is 0.09º, 0.47º and 0.27º for the BSC222 thin films on STO (1 0 0), (1 1 0) and (1 1 1) substrates, respectively, indicating the excellent c-axis orientation. The difference of the FWHM may be related to the different lattice mismatch between the thin film and the substrate.

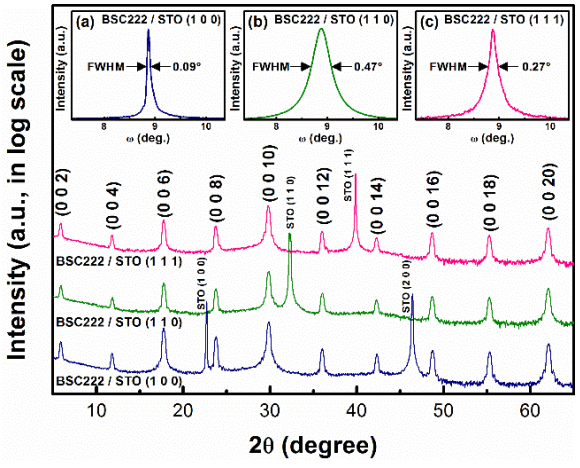


**Fig. 1** HR-XRD patterns of the BSC222 thin films on different substrates. The inset (a), (b) and (c) show the rocking curves of BSC222 (0 0 6) planes for all derived thin films.

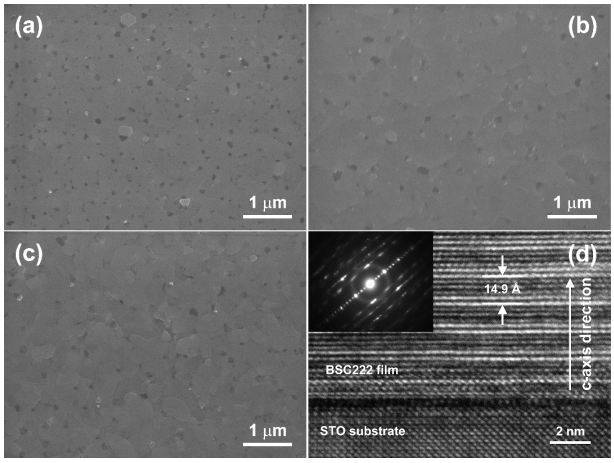


**Fig. 2** Surface FE-SEM images for the BSC222 thin films on STO (a) (1 0 0), (b) (1 1 0) and (c) (1 1 1) substrates; (d) cross-sectional HR-TEM image for the BSC222 thin film on STO (1 0 0) substrate, and the inset shows the corresponding selected-area electron diffraction pattern.

Figure 2(a)–(c) present the field-emission scanning electron microscopy (FE-SEM) images to give the surface morphology for all derived films. It is seen that all BSC222 thin films are quite dense. Fig. 2(d) gives the cross-sectional high-resolution transmission electron microscopy (HR-TEM) in the vicinity of the film-substrate interface for the BSC222 film on the STO (1 0 0) substrate (the HR-TEM results for the other two thin films show similar results and are not shown here). It can be clearly seen that periodical lattice strips perpendicular to the c-axis are regular. The measured c-axis lattice constant is about 14.9 Å, which is same as the XRD results. Also, the selected-area electron diffraction patterns (SAED) is shown in the inset of Fig. 2(d), confirming the c-axis self-orientation.

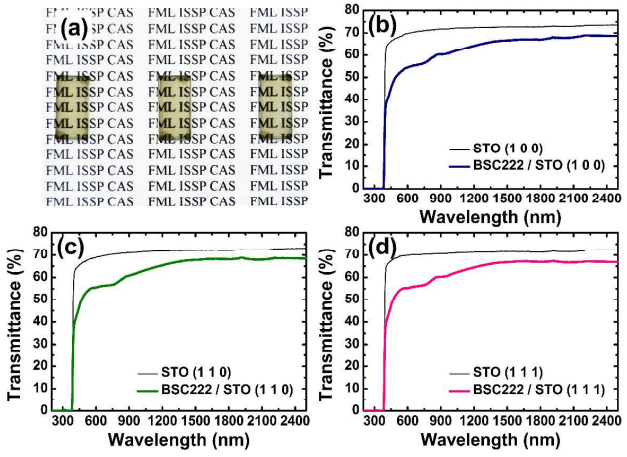


**Fig. 3** (a) Photograph of the transparent BSC222 thin films on a paper with background of letters (from left to right are the thin films on STO (1 0 0), (1 1 0) and (1 1 1) substrates, respectively); (b)–(d) transmittance measurements of all STO substrates and BSC222 films on STO substrates.

The photograph for all deposited BSC222 thin films is shown in Fig. 3(a). It is clearly seen that all derived BSC222 thin films are visibly transparent. Transmittance measurements on the BSC222 thin films and the bare STO substrates are illustrated in Fig. 3(b)–(d). It is interesting to observe that the BSC222 thin films are transparent in the visible range, and the transmittance at 800 nm is about 58% for all derived thin films, which is similar to the previous reports about p-type delafossite thin films.[20,21] With increasing of wavelength, in the near infrared region, the optical transmittances of BSC222 thin films on STO substrates are significantly enhanced as compared with in the visible range. It reaches as high as 68% for photo wavelengths longer than 1500 nm. In order to reveal the intrinsic transmittance for BSC222 thin films, we subtract the transmittance of substrates according to the ratio $T_{total}/T_{substrate}$ ($T_{total}$ and $T_{substrate}$ refer to the measured transmittance for BSC222 thin film deposited on STO substrate and bare STO substrate, respectively). It shows that the ratios of BSC222 on STO (1 0 0), STO (1 1 0) and STO (1 1 1) at 1500 nm are 92%, 94% and 93%, respectively, indicating very high light transmission in the near infrared region. Moreover, the relationship between the optical absorption coefficient ($\alpha$) and the photo energy ($h\nu$) can be described by the equation, $\alpha h\nu = A(h\nu - E_g)^m$, where $A$ and $E_g$ are a constant and the optical band gap width of the material, respectively.[8] Here, the correlation between $(\alpha h\nu)^m$ and $h\nu$ can be well linear fitted when the exponent $m$ is 1/2, indicating a direct band gap of the BSC222 thin films. The optical band gap width is about 3.21 eV according to the fitting results for all derived BSC222 thin films (not shown here). Furthermore, it is found that the transmittance of BSC222 thin films deposited on STO substrates and the bare STO substrates show an opaque characteristic in the ultraviolet region. Besides, it can be seen that the substrate crystal orientation has a little influence on the transmittance of the BSC222 thin films.

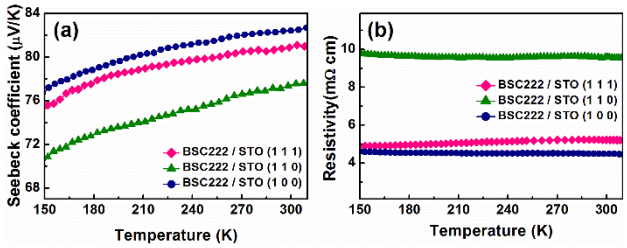


**Fig. 4** Temperature dependence of (a) Seebeck coefficient and (b) resistivity for all derived thin films.

Figure 4(a) gives the temperature dependent Seebeck coefficient ($S$) for all BSC222 thin films. The positive Seebeck coefficient suggests that the major charge carriers are holes (p-type). Moreover, Fig. 4(b) shows the electrical transport properties of all BSC222 thin films on STO substrate. It is worth to mentioned here that the resistivity of BSC222 thin film on STO (1 0 0) substrate is about 4.5 mΩ cm (conductivity, $\sigma \approx 222$ S cm$^{-1}$) at room temperature, which is the lowest value in resistivity (highest value in conductivity) for p-type TCOs.[14] Room temperature Hall measurements show that the carrier concentration ($n$) are $1.29 \times 10^{21}$, $1.01 \times 10^{21}$, and $1.15 \times 10^{21}$ cm$^{-3}$, and carrier mobility ($\mu$) are 1.07, 0.64, and 1.03 cm$^2$ V$^{-1}$s$^{-1}$ for BSC222 thin films on STO (1 0 0), STO (1 1 0), and STO (1 1 1) substrates, respectively. In layered cobaltates, it is well known that the variation of Seebeck coefficient can be elucidated using the Mott formula, $S = c_e/n + (\pi^2 k_B{}^2 T/3e)[\partial \ln\mu(\varepsilon)/\partial\varepsilon]$, where $c_e$, $n$, $k_B$, and $\mu(\varepsilon)$ are the electronic-specific heat, carrier concentration, Boltzmann constant and energy correlated carrier mobility, respectively.[22] The BSC222 thin film on STO (1 0 0) substrate shows the largest Seebeck coefficient maybe mainly due to its largest carrier mobility according to the Mott formula, even though it has the largest carrier concentration among the three different thin films. Also, it presents

the lowest resistivity can be easily explained by the resistivity expression $\rho = 1/ne\mu$. Moreover, the effect of the out-of-plane orientation (see the insets of Fig. 1) on Seebeck coefficient and resistivity cannot be neglected. Anyway, it is confirmed that all derived BSC222 thin films have a p-type conducting behavior with low resistivity.

**Table 1** Room temperature resistivity, Seebeck coefficient, sheet resistance, average transmittance in the visible range and calculated figure of merit for all BSC222 thin films on STO substrates

| BSC222 film | $\rho$ (300K) (mΩ cm) | $S$ (300K) (μV/K) | $R_{sh}$ (300K) (kΩ) | $T_{avg.}$ (%) | $FOM$ ($M\Omega^{-1}$) |
|---|---|---|---|---|---|
| on STO (1 0 0) | 4.5 | 82 | 1.8 | 50 | 800 |
| on STO (1 1 0) | 9.6 | 78 | 3.8 | 51 | 395 |
| on STO (1 1 1) | 5.2 | 81 | 2.1 | 51 | 715 |

In general, the value of *FOM* is used to evaluate the performance of the transparent conducting thin films since the high optical transmission and electrical conductivity are conflicting properties. Room temperature $R_{sh}$, average optical transmittance ($T_{avg.}$) in the visible range (calculated with the same photon energies as Ref [4]) and the corresponding *FOM* for all thin films are shown in Table 1. Surprisingly, the value of *FOM* for all BSC222 thin film on STO (1 0 0), STO (1 1 0) and STO (1 1 1) is 800, 395, 715 $M\Omega^{-1}$, respectively. These values are the highest for p-type transparent conducting thin films by solution methods.[14]

In summary, c-axis self-oriented BSC222 thin films are first reported as novel p-type transparent conducting thin films. The usage of a chemical solution method is suitable for large scalable in preparation. The values of *FOM* for all derived BSC222 thin films are the highest in solution-derived p-type transparent conducting thin films. The maximum *FOM* can reach as high as 800 $M\Omega^{-1}$, indicating the BSC222 thin film is a promising candidate for p-type TCOs.

This work was supported by the National Basic Research Program of China under contract No. 2014CB931704. Dr. H. Luo acknowledges the funding support from NSF under Grant No. 1131290. In particular, we thank Dapeng Cui, Dingfu Shao and Shu Zhou for photograph and technical assistance.

## Notes and references

[a] Key Laboratory of Materials Physics, Institute of Solid State Physics, Chinese Academy of Sciences, Hefei 230031, China.
E-mail: xbzhu@issp.ac.cn, ypsun@issp.ac.cn
[b] Department of Chemical Engineering, New Mexico State University, Las Cruces, New Mexico 88003, USA.
[c] High Magnetic Field Laboratory, Chinese Academy of Sciences, Hefei 230031, China.

† Electronic Supplementary Information (ESI) available: Details of experimental procedures and characterization. See DOI: 10.1039/b000000x/

1 H. Kawazoe, M. Yasukawa, H. Hyodo, M. Kurita, H. Yanagi and H. Hosono, *Nature*, 1997, **389**, 939–942.
2 M.-K. Lee and Y.-T. Lai, *J. Phys. D: Appl. Phys.*, 2013, **46**, 055109.
3 H. Luo, M. Jain, T. M. McCleskey, E. Bauer, A. K. Burrell and Q. Jia, *Adv. Mater.*, 2007, **19**, 3604–3607.
4 E. Arca, K. Fleischer and I. V. Shvets, *Appl. Phys. Lett.*, 2011, **99**, 111910.
5 E. Fortunato, P. Barquinha and R. Martins, *Adv. Mater.*, 2012, **24**, 2945–2986.
6 S. Sheng, G. Fang, C. Li, S. Xu and X. Zhao, *Phys. Stat. Sol. A*, 2006, **203**, 1891–1900.
7 G. Hautier, A. Miglio, G. Ceder, G.-M. Rignanese and X. Gonze, *Nat. Commun*, 2013, **4**, 2292.
8 P. Zhai, Q. Yi, J. Jian, H. Wang, P. Song, C. Dong, X. Lu, Y. Sun, J. Zhao, X. Dai, Y. Lou, H. Yang and G. Zou, *Chem. Commun.*, 2014, **50**, 1854–1856.
9 J. He, Y. Liu and R. Funahashi, *J. Mater. Res.*, 2011, **26**, 1762.
10 H.-H. Wang, D.-F. Cui, S.-Y. Dai, H.-B. Lu, Y.-L. Zhou, Z.-H. Chen and G.-Z. Yang, *J. Appl. Phys.*, 2001, **90**, 4664.
11 Y. Ando, N. Miyamoto, K. Segawa, T. Kawata and I. Terasaki, *Phys. Rev. B*, 1999, **60**, 10580.
12 P. Limelette, V. Hardy, P. Auban-Senzier, D. Jérome, D. Flahaut, S. Hébert, R. Frésard Ch. Simon, J. Noudem and A. Maignan, *Phys. Rev. B*, 2005, **71**, 233108.
13 R. Wei, H. Jian, X. Tang, J. Yang, L. Hu, L. Chen, J. Dai, X. Zhu and Y. Sun, *J. Am. Ceram. Soc.*, 2013, **96**, 2396–2401.
14 M. Aksit, S. K. Kolli, I. M. Slauch and R. D. Robinson, *Appl. Phys. Lett.*, 2014, **104**, 161901.
15 T. Sun, H. H. Hng, Q. Y. Yan and J. Ma, *J. Appl. Phys.*, 2010, **108**, 083709.
16 A. C. Masset, C. Michel, A. Maignan, M. Hervieu, O. Toulemonde, F. Studer, B. Raveau and J. Hejtmanek, *Phys. Rev. B*, 2000, **62**, 166.
17 X. Zhu, D. Shi, S. Dou, Y. Sun, Q. Li, L. Wang, W. Li,W. Yeoh, R. Zheng, Z. Chen and C. Kong, *Acta Mater.*, 2010, **58**, 4281–4291.
18 X. Zhu, X. Tang, D. Shi, H. Jian, H. Lei, W. K. Yeoh, B. Zhao, J. Yang, Q. Li, R. Zheng, S. Dou and Y. Sun, *Dalton Trans.*, 2011, **40**, 9544–9550.
19 S. Wang, Z. Zhang, L. He, M. Chen, W. Yu and G. Fu, *Appl. Phys. Lett*, 2009, **94**, 162108.
20 S. H. Lim, S. Desu and A. C. Rastogi, *J. Phys. Chem. Solids*, 2008, **69**, 2047–2056.
21 R. Nagarajan, A. D. Draeseke, A. W. Sleight and J. Tate, *J. Appl. Phys*, 2001, **89**, 8022.
22 B. Fisher, L. Patlagan, G. Reisner, and A. Knizhnik, *Phys. Rev. B*, 2000, **61**, 470.